Optimization of partial-state feedback for vibratory energy harvesters subjected to broadband stochastic disturbances

2011 Smart Mater. Struct. 20 085019

(http://iopscience.iop.org/0964-1726/20/8/085019)

Smart Mater. Struct. **20** (2011) 085019 (13pp) doi:10.1088/0964-1726/20/8/085019

Optimization of partial-state feedback for vibratory energy harvesters subjected to broadband stochastic disturbances

Ian L Cassidy[1], **Jeffrey T Scruggs**[1] **and Sam Behrens**[2]

[1] Department of Civil and Environmental Engineering, Duke University, Box 90287, Durham, NC 27708, USA
[2] CSIRO Energy Centre, PO Box 330, Newcastle, New South Wales 2300, Australia

E-mail: ian.cassidy@duke.edu, jeff.scruggs@duke.edu and sam.behrens@csiro.au

Received 22 March 2011, in final form 26 May 2011
Published 19 July 2011
Online at stacks.iop.org/SMS/20/085019

Abstract
In many applications of vibratory energy harvesting, the external disturbance is most appropriately modeled as a broadband stochastic process. Optimization of the average power generated from such disturbances is a feedback control problem, and solvable via LQG (linear–quadratic–Gaussian) control theory. Implementing the optimal feedback controller requires a power electronic drive capable of two-way power flow, which can impose dynamic relationships between the voltage and current of the transducer. Determining the optimal energy harvesting current control is accomplished by solving a nonstandard Riccati equation. In this paper we show that appropriate tuning of the passive parameters in the harvesting system results in a decoupled solution to the Riccati equation and a corresponding controller that only requires half of the states for feedback. However, even when such tuning methods are not used and the solution to the Riccati equation does not decouple, it is possible to determine the states in the feedback law that contribute the most to the average power generated by the harvester. As such, partial-state feedback gains can be optimized using a gradient descent method. Two energy harvesting examples are presented, including a single-degree-of-freedom oscillator with an electromagnetic actuator and a piezoelectric bimorph cantilever beam, to demonstrate these concepts.

1. Introduction

Electromechanical systems to harvest vibratory energy have been the subject of considerable research activity over the last decade, with the focus being primarily on low-power applications requiring energy autonomy, such as wireless sensing and embedded computing systems [1–4]. A typical vibratory energy harvester relies on a passive electromechanical system, which consists of a flexible mechanical structure with embedded transducers, to generate power from an exogenous disturbance. The transducers must be interfaced with a power electronic network that extracts power and delivers it to a storage device, such as a rechargeable battery or a supercapacitor.

The single-directional DC/DC converter in figure 1(a), and variants thereof, has gained a significant amount of attention for low-power energy harvesting applications [5–7]. This particular circuit is called a buck–boost converter due to the fact that it can make the output voltage magnitude less than or greater than the input voltage magnitude. Power flow in such converters is regulated via high-frequency pulse-width modulation (PWM) switching control of the MOSFETs in the circuitry. Single-directional DC/DC converters are advantageous in small-scale applications, because they only require that a single MOSFET be switched, thus reducing gating losses. However, for applications where the parasitic losses are small in comparison to the average power generated, the single-directional power flow capability of these converters can hamper their ability to optimize power generation from stochastic dynamical responses, as illustrated in [8].

In Ottman *et al* [9], they experimentally demonstrated the operation of a buck converter to extract power from a piezoelectric transducer, and proposed that for such applications, it was advantageous to operate the converter in the discontinuous conduction regime. Subsequent studies for buck–boost converters in discontinuous conduction have

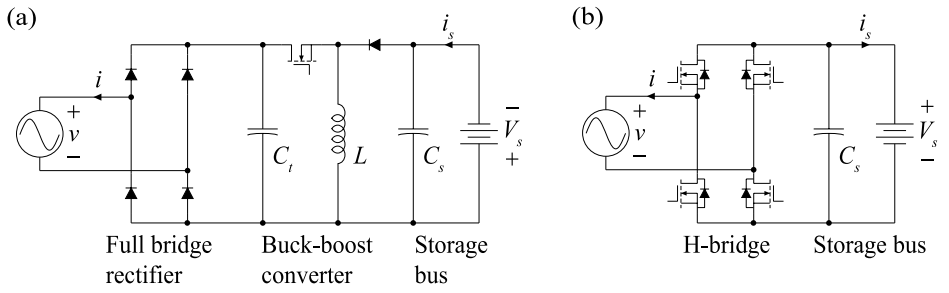

Figure 1. Energy harvesting converters interfaced with a storage bus; (a) full bridge rectifier connected to a buck–boost converter; (b) H-bridge.

been examined by Lefeuvre *et al* [6] and later by Kong *et al* [7]. In this regime, the inductor fully demagnetizes (i.e., its current drops to zero) before the end of the switching cycle, and remains so until the converter's MOSFET is gated on again at the leading edge of the next switching cycle. Operation of a buck–boost converter in discontinuous conduction results in an input admittance which is decoupled from the behavior of the storage voltage. Furthermore, if the transducer side capacitance, C_t, is sufficiently small, and possibly with supplemental input filtering, then the admittance is approximately linear and resistive in low- to mid-frequency bands, with the value of the effective resistance being proportional to the inverse square of the switching duty cycle. As such, the design of these converters for optimal operation proceeds by first determining the effective shunt resistance which maximizes power generation from the transducer, and then synthesizing the duty cycle from this resistance.

For energy harvesting applications in which the disturbance is concentrated at a single frequency, such converters can be incorporated into a larger passive network and can be tuned to optimize power generation. As pointed out in [8, 10], power generation is optimized by matching the input admittance of the effective passive network (including the effective resistance of the converter) to the complex conjugate transpose of the harvester admittance at this frequency. In many applications, the additional passive components required to facilitate this matching condition (such as the inductance necessary to do so for piezoelectric applications) are too large to be practical, which has given rise to the use of various nonlinear active circuits based on synchronized switching concepts [11–14], which are used to actively correct the power factor of the transducer at the frequency of excitation.

However, for cases in which the disturbance is modeled as a stochastic process, optimization of the dynamic behavior of the electronics for maximal power generation is more challenging. It has been shown in [8] that maximizing the power generated from an energy harvester using the same impedance matching techniques mentioned above, always results in an anti-causal admittance. That study also showed that an optimal causality-constrained admittance does exist, and that it can be determined using LQG control theory. Another approach for determining admittances for this class of problems has been proposed by Adhikari *et al* [15]. That study uses a Laplace-domain analysis to determine the analytical expression for the resistance that maximizes the mean power harvested from a piezoelectric beam subjected to a stationary white noise disturbance.

For the stochastic case, Scruggs showed in [8] that if the electronics of energy conversion are efficient enough, then the optimal causal control of transducer current (as derived by LQG theory) cannot be realized with a passive network. This is because in such circumstances, there are frequency bands in which the average power for the optimized system flows the other way; i.e., from storage back into the harvester. That study advocates the realization of a synthetic dynamic admittance using a two-way (i.e., four-quadrant) power electronic converter. One example of such a converter, called an H-bridge, is shown in figure 1(b). Operation of the H-bridge requires control of four MOSFETs and thus requires more parasitic power than a one-directional converter, which is the price paid for two-way directionality of power flow. Many previous studies have used H-bridge drives for various piezoelectric applications, e.g., [16, 17], including their proposed use in piezoelectric energy harvesting applications [18, 19]. H-bridge control of currents for electromagnetic transducers is standard, and their use in electromagnetic energy harvesting applications has been investigated in [20]. Irrespective of the application, the drive has to be capable of high-bandwidth current tracking. This technology is well understood and can be accomplished using hysteretic switching or PWM techniques [21].

For stochastic energy harvesting applications the theoretically optimal power generation current is a feedback function of the system response, including the transducer voltage, as well as other response states that may be available via sensor feedback. Allowable complexity of this algorithm depends on the hardware used to realize it, which in turn depends on the scale of the problem. More complex algorithms must be realized via a microprocessor or programmable controller, and for problems in which transduction power is low, such implementations may demand static power consumption levels comparable with transduction power levels. In such applications, it is therefore useful to simplify feedback algorithms to decision processes that can be realized using simple analog networks, containing as few active components as possible. This observation leads to an interesting connection between stochastic energy harvesting problems, and fixed-structure and static control synthesis concepts.

Motivated by the above observation, the primary contributions of this paper are twofold. First, building upon the techniques developed in [8, 19] and the results

presented in [22], we first show that for stochastic disturbances characterized by second-order, bandpass-filtered white noise, energy harvesters can be passively 'tuned' such that optimal stationary power generation only requires half of the system states for feedback in the active circuit. Interestingly, these states are the ones most easy to sense. For example, for a base-excited SDOF electromagnetic harvester, only the disturbance acceleration and transducer voltage are needed for feedback. For base-excited piezoelectric bimorph transducers with one predominant mode, and with appropriate passive electrical tuning, the only necessary feedback quantities are the disturbance acceleration and transducer voltage, together with the mechanical velocity. One can view these tuning techniques as a 'stochastic counterpart' to the tuning techniques used in harvesting applications characterized by monochromatic disturbances. In such cases, electrical tuning techniques can be used to maximize harvested power at the excitation frequency using only transducer voltage feedback, resulting in a harvesting circuit with a resistive input impedance. By contrast, even with the use of tuning techniques, optimal power generation in a stochastic context appears to almost always require knowledge of other quantities in addition to transducer voltage.

The fact that only half the states are required for feedback in tuned harvesters is a by-product of a special structure which arises in the matrix solution to the associated Riccati equation used to synthesize the optimal feedback gains. In effect, the passive tuning techniques have the effect of causing many of the entries in this matrix to be identically zero. However, in many applications such tuning techniques may be impractical, due, for example, to the large inductances they often require for piezoelectric applications. In other applications, even with the tuning techniques implemented as described, it may not be practical to feed back the reduced subset of system states required for optimality. Motivated by this observation, the second contribution of the paper is the application of fixed-structure feedback optimization techniques to maximize power generation for the case in which the availability of various system states for feedback is fixed in the design. For this case, we assume that the transducer current is determined based only on concurrent measurements of a set of prescribed states (i.e., the feedback law is presumed to be static), resulting in a decision process which can be realized with a very simple and efficient analog circuit.

2. Disturbance and harvester models

For this discussion, we consider the case in which the disturbance acceleration $a(t)$ is modeled as filtered noise. We will assume that $a(t)$ has a power spectral density equal to

$$\Phi_{\mathrm{a}}(\omega) = \left| \frac{q\mathrm{j}\omega}{-\omega^2 + 2\omega_{\mathrm{a}}\zeta_{\mathrm{a}}\mathrm{j}\omega + \omega_{\mathrm{a}}^2} \right|^2 \tag{1}$$

where ω_{a} is the center of the passband of $a(t)$, and ζ_{a} determines the spread of its frequency content. For such a process, it is straightforward to represent the disturbance dynamics by a two-dimensional state space of the form

$$\frac{\mathrm{d}}{\mathrm{d}t}\mathbf{x}_{\mathrm{a}}(t) = \mathbf{A}_{\mathrm{a}}\mathbf{x}_{\mathrm{a}}(t) + \mathbf{B}_{\mathrm{a}}w(t), \tag{2a}$$

$$a(t) = \mathbf{C}_{\mathrm{a}}\mathbf{x}_{\mathrm{a}}(t) \tag{2b}$$

where $w(t)$ is a white noise process with spectral intensity equal to unity. The parameter q in equation (1) is adjusted such that irrespective of ω_{a} and ζ_{a}, $a(t)$ has a consistent standard deviation of σ_{a}; i.e.,

$$\sigma_{\mathrm{a}} = \sqrt{\frac{1}{2\pi}\int_{-\infty}^{\infty} \Phi_{\mathrm{a}}(\omega)\,\mathrm{d}\omega}. \tag{3}$$

This allows us to compare disturbances of varying spectral content, but equal intensity. We refer to the 'narrowband limit' for the disturbance model as the case in which $\zeta_{\mathrm{a}} \to 0$. Similarly, refer to 'broadband limit' as the case in which $\zeta_{\mathrm{a}} \to \infty$.

We assume the harvester is a dissipative system and that the harvester dynamics can be approximated by a finite-dimensional linear state space. Let $H_{\mathrm{a}}(s)$ and $H_i(s)$ be the transfer functions from the disturbance acceleration $a(t)$ and the control current $i(t)$ to the voltage generated by the system $v(t)$, respectively. We will assume both $H_{\mathrm{a}}(s)$ and $H_i(s)$ to be strictly proper and that $H_i(s)$ is weakly strictly positive real (WSPR) [23]. With these assumptions, there always exists a self-dual state space realization [24] for the harvester, of the form

$$\frac{\mathrm{d}}{\mathrm{d}t}\mathbf{x}_{\mathrm{h}}(t) = \mathbf{A}_{\mathrm{h}}\mathbf{x}_{\mathrm{h}}(t) + \mathbf{B}_{\mathrm{h}}i(t) + \mathbf{G}_{\mathrm{h}}a(t), \tag{4a}$$

$$v(t) = \mathbf{B}_{\mathrm{h}}^{\mathrm{T}}\mathbf{x}_{\mathrm{h}}(t). \tag{4b}$$

This representation implies that $H_i(s) = \mathbf{B}_i^{\mathrm{T}}(s\mathbf{I} - \mathbf{A}_{\mathrm{h}})^{-1}\mathbf{B}_i$ and $H_{\mathrm{a}}(s) = \mathbf{B}_i^{\mathrm{T}}(s\mathbf{I} - \mathbf{A}_{\mathrm{h}})^{-1}\mathbf{B}_{\mathrm{a}}$. In the above realization, the total dissipation in the harvester at time t is $-\frac{1}{2}\mathbf{x}_{\mathrm{h}}^{\mathrm{T}}(t)[\mathbf{A}_{\mathrm{h}} + \mathbf{A}_{\mathrm{h}}^{\mathrm{T}}]\mathbf{x}_{\mathrm{h}}(t) \geqslant 0$, and the total energy stored in the harvester is $\frac{1}{2}\mathbf{x}_{\mathrm{h}}^{\mathrm{T}}(t)\mathbf{x}_{\mathrm{h}}(t)$. The WSPR assumption allows us to assume that the pair $(\mathbf{A}_{\mathrm{h}}, \mathbf{A}_{\mathrm{h}} + \mathbf{A}_{\mathrm{h}}^{\mathrm{T}})$ is observable, which implies that no response of the harvester can exhibit zero internal dissipation over any finite interval.

Combining the disturbance and harvester dynamics into an augmented state space yields

$$\frac{\mathrm{d}}{\mathrm{d}t}\mathbf{x}(t) = \mathbf{A}\mathbf{x}(t) + \mathbf{B}i(t) + \mathbf{G}w(t), \tag{5a}$$

$$v(t) = \mathbf{B}^{\mathrm{T}}\mathbf{x}(t) \tag{5b}$$

where the augmented matrices $\mathbf{A}$, $\mathbf{B}$, and $\mathbf{G}$ are

$$\mathbf{A} = \begin{bmatrix} \mathbf{A}_{\mathrm{h}} & \mathbf{G}_{\mathrm{h}}\mathbf{C}_{\mathrm{a}} \\ \mathbf{0} & \mathbf{A}_{\mathrm{a}} \end{bmatrix}, \qquad \mathbf{B} = \begin{bmatrix} \mathbf{B}_{\mathrm{h}} \\ \mathbf{0} \end{bmatrix}, \qquad \mathbf{G} = \begin{bmatrix} \mathbf{0} \\ \mathbf{B}_{\mathrm{a}} \end{bmatrix} \tag{6}$$

and the resultant augmented state vector is $\mathbf{x}(t) = [\,\mathbf{x}_{\mathrm{h}}^{\mathrm{T}}(t) \quad \mathbf{x}_{\mathrm{a}}^{\mathrm{T}}(t)\,]^{\mathrm{T}}$. We make the assumption that $(\mathbf{A}, \mathbf{B}^{\mathrm{T}})$ is observable and $(\mathbf{A}, [\mathbf{B}\ \mathbf{G}])$ is controllable. If this is not the case for the original system model, we assume that the dimension of the augmented state space has been reduced to a minimal realization.

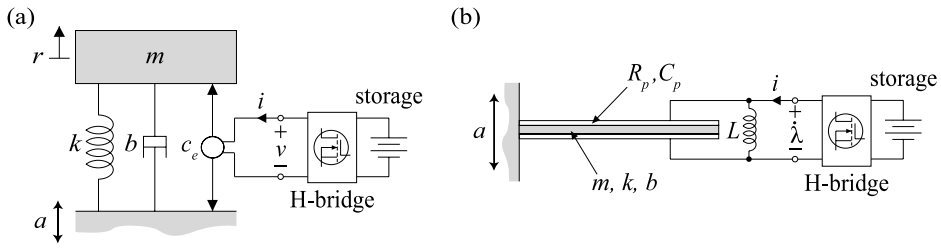

Figure 2. Passive energy harvesting systems: (a) SDOF oscillator with an electromagnetic actuator; (b) piezoelectric bimorph cantilever beam with an inductor connected in parallel.

3. Examples

We now introduce two example systems that will be the focus of the analysis for the remaining sections. The first involves electromagnetic transduction, while the second involves piezoelectric transduction. These two systems are shown in figure 2.

3.1. Electromagnetic example

Consider the single-degree-of-freedom (SDOF) resonant oscillator with mass m, damping b, and stiffness k in figure 2(a). A transducer is attached between the base and the moving mass such that $f_e(t) = c_e i(t)$ where c_e is the coupling coefficient. This system corresponds to an energy harvester with electromagnetic coupling. Similar electromagnetic energy harvesting systems have been demonstrated in [20, 25, 26].

In order to generalize the analysis, we will relate time t to a nondimensional time τ as

$$t = \sqrt{\frac{m}{k}}\tau \tag{7}$$

and will relate the physical variables of the problem to nondimensionalized versions (denoted by overbars) as

$$r(t) = \left(\frac{m\sigma_a}{k}\right)\bar{r}(\tau) \tag{8}$$

$$a(t) = \sigma_a \bar{a}(\tau), \tag{9}$$

$$i(t) = \left(\frac{m\sigma_a}{c_e}\right)\bar{i}(\tau), \tag{10}$$

$$v(t) = \left(c_e\sigma_a\sqrt{\frac{m}{k}}\right)\bar{v}(\tau), \tag{11}$$

where σ_a is the standard deviation of the disturbance acceleration as defined in equation (3). We define the harvester state vector $\mathbf{x}_h(\tau) = [\bar{r}(\tau)\ \bar{\dot{r}}(\tau)]^T$ and it then follows that

$$\mathbf{A}_h = \begin{bmatrix} 0 & 1 \\ -1 & -d \end{bmatrix}, \qquad \mathbf{B}_h = \begin{bmatrix} 0 \\ 1 \end{bmatrix}, \qquad \mathbf{G}_h = \begin{bmatrix} 0 \\ 1 \end{bmatrix} \tag{12}$$

where $d = b/\sqrt{mk}$.

The power spectrum of $\bar{a}(\tau)$ is as in equation (1), but in terms of normalized frequency $\bar{\omega} = \omega\sqrt{m/k}$ and associated normalized parameters $\{\bar{\omega}_a, \bar{q}\}$. We assume that the harvester has been tuned such that its natural frequency is in the center of the disturbance passband, resulting in the normalized matching condition $\bar{\omega}_a = 1$. The quantity $\bar{q}$ chosen such that $\int_{-\infty}^{\infty} \Phi_{\bar{a}}(\bar{\omega})\,d\bar{\omega} = 1$. It turns out that the value of $\bar{q}$ which brings this about is $\bar{q} = 2\sqrt{\zeta_a}$. Augmenting the harvester and disturbance states, the system parameter matrices in equation (5*a*) are

$$\mathbf{A} = \begin{bmatrix} 0 & 1 & 0 & 0 \\ -1 & -d & 0 & 1 \\ 0 & 0 & 0 & 1 \\ 0 & 0 & -1 & -2\zeta_a \end{bmatrix}, \qquad \mathbf{B} = \begin{bmatrix} 0 \\ 1 \\ 0 \\ 0 \end{bmatrix}, \qquad \mathbf{G} = \begin{bmatrix} 0 \\ 0 \\ 0 \\ 2\sqrt{\zeta_a} \end{bmatrix}. \tag{13}$$

3.2. Piezoelectric example

Consider the piezoelectric bimorph cantilever beam in figure 2(b). The transducer has an equivalent capacitance C_p and dielectric leakage resistance R_p. We assume that the deflection at the end of the cantilever beam can be modeled by a finite summation of Galerkin mode shapes. As such, the differential equations describing the dynamics of the beam can be approximated through a standard Rayleigh–Ritz projection. Keeping only the fundamental vibratory mode, we approximate the beam by a mass m, a stiffness k, and a coupling coefficient θ. In addition, a Rayleigh damping term b is assumed for the beam. As seen in figure 2(b) the terminals of the piezoelectric patch are connected in parallel to an inductor with inductance L. Given the assumptions about the dynamics of the beam, the governing equations for this system are

$$m\ddot{r}(t) + b\dot{r}(t) + kr(t) = \Gamma a(t) - \theta\dot{\lambda}(t), \tag{14a}$$

$$C_p\ddot{\lambda}(t) + \frac{1}{R_p}\dot{\lambda}(t) + \frac{1}{L}\lambda(t) = i(t) + \theta\dot{r}(t) \tag{14b}$$

where $\lambda(t)$ is the flux linkage across the piezoelectric patch, $r(t)$ is the relative displacement of the beam, and Γ is an equivalent mass term. Furthermore, we have that the transducer voltage is $v(t) = \dot{\lambda}(t)$.

We nondimensionalize t and r the same way as for the electromagnetic example (i.e., equations (7) and (8) respectively) and further nondimensionalize the remaining dynamic quantities as

$$\lambda(t) = \left(\frac{m\sigma_a}{k}\sqrt{\frac{m}{C_p}}\right)\bar{\lambda}(\tau), \tag{15}$$

$$a(t) = \left(\frac{m\sigma_a}{\Gamma}\right)\bar{a}(\tau), \tag{16}$$

$$i(t) = \left(\theta\sigma_a\sqrt{\frac{m}{k}}\right)\bar{i}(\tau). \tag{17}$$

The nondimensionalized harvester model then has the second-order differential equation

$$\ddot{\mathbf{q}}(\tau) + \mathbf{D}\dot{\mathbf{q}}(\tau) + \mathbf{S}\mathbf{q}(\tau) = \mathbf{B}_1\bar{i}(\tau) + \mathbf{B}_2\bar{a}(\tau) \tag{18}$$

where $\mathbf{q}(\tau) = [\bar{r}(\tau)\,\bar{\lambda}(\tau)]^{\mathrm{T}}$ and the coefficient matrices are

$$\mathbf{D} = \begin{bmatrix} d & 1 \\ -1 & \beta \end{bmatrix}, \qquad \mathbf{S} = \begin{bmatrix} 1 & 0 \\ 0 & \alpha \end{bmatrix}, \qquad \mathbf{B}_1 = \begin{bmatrix} 0 \\ 1 \end{bmatrix}, \qquad \mathbf{B}_2 = \begin{bmatrix} 1 \\ 0 \end{bmatrix}. \tag{19}$$

In the above, the mechanical damping d remains unchanged from the previous example, while the electrical damping β is

$$\beta = \frac{1}{C_p R_p}\sqrt{\frac{m}{k}} \tag{20}$$

and α is the ratio of the squared natural frequencies of the electrical and mechanical subsystems; i.e.,

$$\alpha = m/kC_pL. \tag{21}$$

We assume that the state space describing the disturbance dynamics is the same as the state space defined in the previous example. Thus, we have that the augmented state space characterizing the piezoelectric harvester and disturbance dynamics can be expressed as

$$\mathbf{A} = \begin{bmatrix} \mathbf{0} & \mathbf{I} & \mathbf{0} & \mathbf{0} \\ -\mathbf{S} & -\mathbf{D} & \mathbf{0} & \mathbf{B}_2 \\ \mathbf{0} & \mathbf{0} & 0 & 1 \\ \mathbf{0} & \mathbf{0} & -1 & -2\zeta_a \end{bmatrix}, \qquad \mathbf{B} = \begin{bmatrix} \mathbf{0} \\ \mathbf{B}_1 \\ 0 \\ 0 \end{bmatrix}, \qquad \mathbf{G} = \begin{bmatrix} \mathbf{0} \\ \mathbf{0} \\ 0 \\ 2\sqrt{\zeta_a} \end{bmatrix}. \tag{22}$$

We will henceforth uniformly assume that the electromagnetic example and the piezoelectric example have been nondimensionalized as described above. To ease the notation, we will do away with all overbars and refer to the nondimensional time as t.

4. Optimal energy harvesting

For the moment, we presume that the entire system state, $\mathbf{x}(t)$ is available for feedback. In this case, the design problem involves the design of a causal feedback law $\mathbf{x} \mapsto i$. The objective is to find the particular feedback law which maximizes the average power generated in stationary stochastic response. To do this, first we define the power delivered to storage as the power extracted from the transducer, minus the transmission losses in the power electronic circuitry. If we approximate these losses as resistive, with some resistance R, then the power delivered to storage is

$$P_s(t) = -i(t)v(t) - Ri^2(t). \tag{23}$$

If we take the expectation of both sides of equation (23), then we can define the average power generated as the expectation of the power delivered to storage; i.e.,

$$\bar{P}_{\mathrm{gen}} = -\mathcal{E}\{i(t)\mathbf{B}^{\mathrm{T}}\mathbf{x}(t) + Ri^2(t)\}. \tag{24}$$

This is equivalent to a LQG optimal control problem. We define the cost function as

$$J = \mathcal{E}\left\{\begin{bmatrix} \mathbf{x}(t) \\ i(t) \end{bmatrix}^{\mathrm{T}}\begin{bmatrix} \mathbf{0} & \frac{1}{2}\mathbf{B} \\ \frac{1}{2}\mathbf{B}^{\mathrm{T}} & R \end{bmatrix}\begin{bmatrix} \mathbf{x}(t) \\ i(t) \end{bmatrix}\right\}. \tag{25}$$

Minimizing the cost function J is equivalent to maximizing $\bar{P}_{\mathrm{gen}}$. Note that the performance functional is sign-indefinite. This reflects the observation that if $i(t)$ is controlled poorly then the efficiency of conversion can be negative, implying drainage of energy from storage rather than accumulation.

We make the assumption that the H-bridge can control the current $i(t)$ with high enough bandwidth such that its dynamics lie outside the frequency band of the disturbance. This assumption may be unjustified in some applications, but for applications with response bandwidths below about 1 kHz, it is often reasonable. Given this assumption, we may view $i(t)$ as a control input which can be regulated as desired. The following theorem then draws the connection between energy harvesting and optimal LQG control. Its proof can be found in [8].

Theorem 1. *Over the space of all causal, continuous feedback functions, the optimal energy harvesting current is characterized by the linear state feedback relationship*

$$i(t) = \mathbf{K}\mathbf{x}(t) \tag{26}$$

where

$$\mathbf{K} = -\frac{1}{R}\mathbf{B}^{\mathrm{T}}\left(\mathbf{P} + \frac{1}{2}\mathbf{I}\right) \tag{27}$$

and $\mathbf{P} = \mathbf{P}^{\mathrm{T}} < 0$ *is the unique, stabilizing solution to the nonstandard Riccati equation*

$$\mathbf{A}^{\mathrm{T}}\mathbf{P} + \mathbf{P}\mathbf{A} - \frac{1}{R}\left(\mathbf{P} + \frac{1}{2}\mathbf{I}\right)\mathbf{B}\mathbf{B}^{\mathrm{T}}\left(\mathbf{P} + \frac{1}{2}\mathbf{I}\right) = \mathbf{0}. \tag{28}$$

The optimal average power generated is

$$\bar{P}_{\mathrm{gen}} = -\mathbf{G}^{\mathrm{T}}\mathbf{P}\mathbf{G}. \tag{29}$$

Implementing the state feedback control law in equation (26) generally requires knowledge of every state in the system. In other words, every component in the feedback gain matrix $\mathbf{K}$ will in general be nonzero. However, it turns out that if the augmented system can be expressed in the realization presented in section 2, then the stabilizing solution $\mathbf{P}$ to the Riccati equation in equation (28) has a special structure. Specifically, $\mathbf{P}$ has several block entries that are equal to zero and several nonzero block entries that are repeated. As a result of this, the solution for $\mathbf{K}$ in equation (27) then has many entries which are also zero. We now present a theorem which formally introduces these concepts. Its proof may be found in appendix B.

Theorem 2. *If the harvester dynamics can be expressed as*

$$\mathbf{A}_\mathrm{h} = \begin{bmatrix} \mathbf{0} & \mathbf{I} \\ -\mathbf{I} & -\mathbf{D} \end{bmatrix}, \qquad \mathbf{B}_\mathrm{h} = \begin{bmatrix} \mathbf{0} \\ \mathbf{B}_1 \end{bmatrix}, \qquad \mathbf{G}_\mathrm{h} = \begin{bmatrix} \mathbf{0} \\ \mathbf{B}_2 \end{bmatrix} \tag{30}$$

and the disturbance dynamics can be expressed as

$$\mathbf{A}_\mathrm{a} = \begin{bmatrix} \mathbf{0} & \mathbf{I} \\ -\mathbf{I} & -\mathbf{Z} \end{bmatrix}, \qquad \mathbf{B}_\mathrm{a} = \begin{bmatrix} \mathbf{0} \\ \mathbf{Q} \end{bmatrix}, \qquad \mathbf{C}_\mathrm{a} = \begin{bmatrix} \mathbf{0} \\ \mathbf{I} \end{bmatrix}^\mathrm{T} \tag{31}$$

then the unique, stabilizing solution to the Riccati equation in equation (28) is

$$\mathbf{P} = \begin{bmatrix} \mathbf{P}_{22} & \mathbf{0} & \mathbf{P}_{24} & \mathbf{0} \\ \mathbf{0} & \mathbf{P}_{22} & \mathbf{0} & \mathbf{P}_{24} \\ \mathbf{P}_{24}^\mathrm{T} & \mathbf{0} & \mathbf{P}_{44} & \mathbf{0} \\ \mathbf{0} & \mathbf{P}_{24}^\mathrm{T} & \mathbf{0} & \mathbf{P}_{44} \end{bmatrix} \tag{32}$$

where $\mathbf{P}_{22}$, $\mathbf{P}_{24}$, *and* $\mathbf{P}_{44}$ *can be solved sequentially as*

$$\mathbf{P}_{22}\mathbf{D} + \mathbf{D}^\mathrm{T}\mathbf{P}_{22} + \frac{1}{R}\left(\mathbf{P}_{22} + \frac{1}{2}\mathbf{I}\right)\mathbf{B}_1\mathbf{B}_1^\mathrm{T}\left(\mathbf{P}_{22} + \frac{1}{2}\mathbf{I}\right) = \mathbf{0}, \tag{33}$$

$$\mathbf{P}_{22}\mathbf{B}_2 - \mathbf{P}_{24}\mathbf{Z} - \mathbf{D}^\mathrm{T}\mathbf{P}_{24} - \frac{1}{R}\left(\mathbf{P}_{22} + \frac{1}{2}\mathbf{I}\right)\mathbf{B}_1\mathbf{B}_1^\mathrm{T}\mathbf{P}_{24} = \mathbf{0}, \tag{34}$$

$$\mathbf{P}_{24}^\mathrm{T}\mathbf{B}_2 + \mathbf{B}_2^\mathrm{T}\mathbf{P}_{24} - \mathbf{P}_{44}\mathbf{Z} - \mathbf{Z}^\mathrm{T}\mathbf{P}_{44} - \frac{1}{R}\mathbf{P}_{24}^\mathrm{T}\mathbf{B}_1\mathbf{B}_1^\mathrm{T}\mathbf{P}_{24} = \mathbf{0}. \tag{35}$$

For the state vector partitioned analogously to $\mathbf{P}$, *the corresponding optimal gain matrix is*

$$\mathbf{K} = [\,\mathbf{0} \quad -\tfrac{1}{R}\mathbf{B}_1^\mathrm{T}(\mathbf{P}_{22} + \tfrac{1}{2}\mathbf{I}) \quad \mathbf{0} \quad -\tfrac{1}{R}\mathbf{B}_1^\mathrm{T}\mathbf{P}_{24}\,] \tag{36}$$

and the optimal power generation is

$$\bar{P}_\mathrm{gen} = -\mathbf{Q}^\mathrm{T}\mathbf{P}_{44}\mathbf{Q}. \tag{37}$$

From this theorem we obtain the interesting result that only half of the states are required for the optimal energy harvesting current.

4.1. Electromagnetic example

Returning to the electromagnetic energy harvesting example, it is clear that the matrices in equation (13) satisfy the conditions in theorem 2. As such, the corresponding decoupled solution to the Riccati equation in equation (32), with scalar quantities P_{22}, P_{24}, and P_{44}, is found by solving equations (33)–(35). Each of these equations is scalar, and their solutions may be solved symbolically in terms of the system parameters, as

$$P_{22} = -(dR + \tfrac{1}{2}) + \sqrt{d^2R^2 + dR}, \tag{38}$$

$$P_{24} = R\frac{-(dR + \frac{1}{2}) + \sqrt{d^2R^2 + dR}}{2\zeta_\mathrm{a}R + \sqrt{d^2R^2 + dR}}, \tag{39}$$

$$P_{44} = \frac{1}{4\zeta_\mathrm{a}}\left(2R\frac{-(dR + \frac{1}{2}) + \sqrt{d^2R^2 + dR}}{2\zeta_\mathrm{a}R + \sqrt{d^2R^2 + dR}} - \left(\frac{-(dR + \frac{1}{2}) + \sqrt{d^2R^2 + dR}}{2\zeta_\mathrm{a}R + \sqrt{d^2R^2 + dR}}\right)^2\right). \tag{40}$$

Thus, we have a symbolic solution for the optimal energy harvesting current; i.e.,

$$i(t) = \left(\frac{dR - \sqrt{d^2R^2 + dR}}{R}\right)v(t) - \left(\frac{-(dR + \frac{1}{2}) + \sqrt{d^2R^2 + dR}}{2R\zeta_\mathrm{a} + \sqrt{d^2R^2 + dR}}\right)a(t) \tag{41}$$

where we have used the fact that $v(t)$ and $a(t)$ are the second and fourth states in $\mathbf{x}(t)$, respectively. Furthermore, we have a symbolic solution for the corresponding optimal harvested power, as

$$\bar{P}_\mathrm{gen} = -2R\frac{-(dR + \frac{1}{2}) + \sqrt{d^2R^2 + dR}}{2R\zeta_\mathrm{a} + \sqrt{d^2R^2 + dR}} + \left(\frac{-(dR + \frac{1}{2}) + \sqrt{d^2R^2 + dR}}{2R\zeta_\mathrm{a} + \sqrt{d^2R^2 + dR}}\right)^2. \tag{42}$$

It is interesting to examine the symbolic dependency of the optimal feedback law on the parameters d, ζ_a, and R. Referring to the gains K_v and K_a in equation (41) (i.e., $i(t) = K_\mathrm{v}v(t) + K_\mathrm{a}a(t)$), we notice that as $R \to 0$, both these gains go to infinity. It is also interesting that K_v is independent of the bandwidth of $a(t)$. Meanwhile, K_a reduces in magnitude from its value for harmonic excitation (with $\zeta_\mathrm{a} = 0$) to the infinite-broadband case, for which $K_\mathrm{a} \to 0$. For the narrowband case, K_a is significantly nonzero, implying that even when $a(t)$ is nearly harmonic, it is still the case that explicit knowledge of $a(t)$ may be leveraged to improve harvesting performance. However, in the limit as $\zeta_\mathrm{a} \to 0$, both $a(t)$ and $v(t)$ become purely sinusoidal, and exactly in phase. (The phase condition is a consequence of the fact that the harvester is assumed to be tuned to the center of the passband for $a(t)$.) Thus, in this limiting case, knowledge of both $v(t)$ and $a(t)$ is redundant, as one is known to be a scaled version of the other. We can therefore conclude that in this case, the optimal $i(t)$ is in fact attained by imposing a static admittance; i.e., $i(t) = K_\mathrm{v}v(t)$. This observation is harmonious with what we expect from approaching the harmonic energy harvesting problem for tuned harvesters from an impedance matching perspective [8].

The optimal average power generated, as expressed in equation (42), is always positive. Furthermore, we see that it increases monotonically as ζ_a decreases. This is to be expected, as it stands to reason that for disturbance models of equal acceleration intensity, ones with more signal strength concentrated near resonance will be easier to harvest energy from. Although it is less obvious from equation (42), it is also the case that the power generation decreases monotonically as R increases. This is also to be expected, as it stands to reason that as the electronics become less efficient, the harvesting potential decreases.

Although the contributions of this paper are primarily theoretical, we pause now to consider the implementation of feedback law equation (41). A diagram depicting one possible implementation is shown in figure 3. It should be noted that the supply power is denoted by V_S while the logic power is denoted by V_L. There are several components in this diagram. The first component is the H-bridge driver, which is used to control the four MOSFETs (Q_1, Q_2, Q_3, and Q_4) in the bridge.

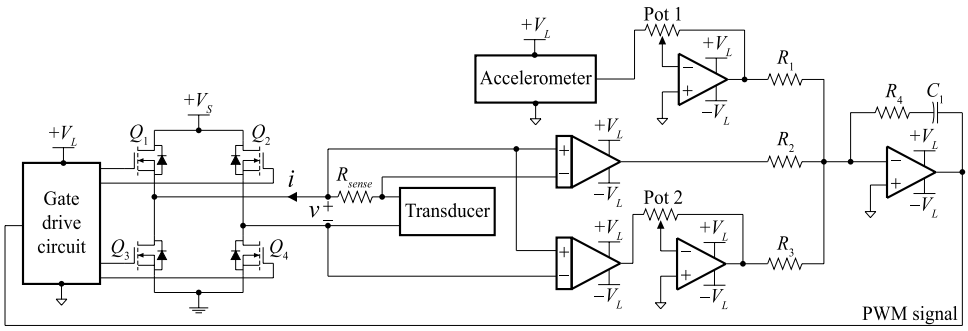

Figure 3. Partial-state feedback circuit diagram consisting of voltage and acceleration measurements with gain adjustment.

A typical H-bridge driver requires two inputs: a PWM signal and a triangle wave signal, which is not pictured. The driver accomplishes tracking of a desired current command signal by switching the MOSFETs on and off at a high frequency using PWM such that the average value of the current imposed across the terminals of the transducer is approximately equal to the command signal.

The next components in this circuit are the voltage, current, and acceleration sensing. The differential voltage across the terminals of the transducer is measured by a simple differential amplifier. Similarly, the current flowing into or out of the transducer can be sensed by measuring the differential voltage across a low resistance sensing resistor, R_{sense}. An accelerometer is attached to the base of the structure and is used to output a voltage signal that is proportional to the disturbance acceleration. Next, the voltage and acceleration signals are sent to two inverting amplifiers that multiply the signals by their respective optimal partial-state gains. These gains can be tuned using two potentiometers (represented by Pot 1 and Pot 2 in figure 3).

The final component in this circuit is a summing amplifier with proportional and integral control in feedback. The voltage signal, acceleration signal, and current signal are summed together to produce the error signal. The error signal then passes through a PI controller, which outputs the PWM signal that is sent to the H-bridge driver. If the chosen resistor values are made such that $R_1 = R_2 = R_3$ then the proportional gain is just $-R_4/R_1$. The integral gain can be adjusted by changing the capacitor value C_1 that is in series with R_4. The values of the proportional and integral gains should be tailored for the particular components used in the circuit as well as the bandwidth constraints on the current command signal.

4.2. Piezoelectric example

Next, we return to the piezoelectric energy harvesting example. The augmented harvester and disturbance model in equation (22) satisfies the conditions in theorem 2 if $\mathbf{S} = \mathbf{I}$, which can be accomplished by setting $\alpha = 1$. Recall that α is the ratio of squared natural frequencies of the mechanical and electrical systems. As such, for a typical piezoelectric energy harvesting system, an extremely large inductor would typically be required for α to equal unity. However, for the purpose of this example, we assume that the value of α is unconstrained and can be tuned via the inductance value L. It turns out that tuning a passive network containing an inductor and a resistor in parallel is exactly what one would do to impedance-match a piezoelectric energy harvester for resonant performance [15].

With $\alpha = 1$, the system model meets the requirements of theorem 2, and the corresponding solution to the Riccati equation thus decouples as in equation (32) (with P_{44} a scalar in this case). We thus can solve for $\mathbf{P}_{22}$, $\mathbf{P}_{24}$, and P_{44} by sequentially solving equations (33)–(35). For this example it is not as easy to find a closed form solution for $\mathbf{P}$, because equation (33) is a 2×2 Riccati equation and $\mathbf{D}$ is a full 2×2 matrix. Nonetheless, in terms of $\mathbf{P}_{22}$ and $\mathbf{P}_{24}$, we find the optimal harvested power is $\bar{P}_{\text{gen}} = -4\zeta_{\text{a}} P_{44}$, and the optimal energy harvesting current is the feedback law is

$$i(t) = -\frac{1}{R}\left[\mathbf{B}_1^{\text{T}}\left(\mathbf{P}_{22} + \frac{1}{2}\mathbf{I}\right)\dot{\mathbf{q}}(t) + \mathbf{B}_1^{\text{T}}\mathbf{P}_{24}a(t)\right] \tag{43}$$

$$= K_{\dot{r}}\dot{r}(t) + K_{\text{v}}v(t) + K_{\text{a}}a(t) \tag{44}$$

with appropriate definitions for $K_{\dot{r}}$, K_{v}, and K_{a}.

5. Energy harvesting via partial-state feedback

We now present a procedure for optimizing the feedback gains corresponding to states that are the most important in terms of the average power generated by the harvester. Since most energy harvesting systems do not satisfy the conditions in theorem 2, they require knowledge of all of the states for optimal power generation. For practical purposes, it is often the case that measuring all of the states is not feasible. Instead, transducer voltage measurements can be passed through a Luenberger observer [27], which is used to estimate the remaining system states. Observer gains can be chosen to achieve close tracking of states, but the construction of a dynamic observer also complicates the feedback circuitry.

It is possible to achieve performance that is almost as good as the optimal full-state upper bound by directly measuring and feeding back only the states that have the most influence on the performance. We have seen in section 4.2 that when the Riccati equation decouples, only the derivatives of the harvester electromechanical coordinates, and the disturbance acceleration (but not its integral) are required for feedback. From this insight we presume that these states have the most influence on performance even when the Riccati equation does not decouple. Furthermore, these states may sometimes be the

easiest to measure. Implementing circuitry to sum static gains of measured states is very simple.

In order to solve for the partial-state feedback gains, we define the output vector $\mathbf{y}(t) = \mathbf{C}\mathbf{x}(t)$. The matrix $\mathbf{C}$ is defined such that $\mathbf{y}(t)$ contains the states that we choose to include for feedback. Without loss of generality, $\mathbf{C}$ will be normalized such that $\mathbf{C}\mathbf{C}^{\mathrm{T}} = \mathbf{I}$. We wish to impose the partial-state feedback law

$$i(t) = \tilde{\mathbf{K}}\mathbf{C}\mathbf{x}(t) \tag{45}$$

where $\tilde{\mathbf{K}}$ is a vector of the optimal partial-state feedback gains. Next, we substitute equation (45) into equation (25), giving

$$J = \mathcal{E}\{\mathbf{x}^{\mathrm{T}}(t)\tilde{\mathbf{Q}}(\tilde{\mathbf{K}})\mathbf{x}(t)\} \tag{46}$$

where

$$\tilde{\mathbf{Q}}(\tilde{\mathbf{K}}) = \tfrac{1}{2}\mathbf{C}^{\mathrm{T}}\tilde{\mathbf{K}}^{\mathrm{T}}\mathbf{B}^{\mathrm{T}} + \tfrac{1}{2}\mathbf{B}\tilde{\mathbf{K}}\mathbf{C} + R\mathbf{C}^{\mathrm{T}}\tilde{\mathbf{K}}^{\mathrm{T}}\tilde{\mathbf{K}}\mathbf{C}. \tag{47}$$

In this case the optimal upper bound on power generation is

$$\bar{P}_{\mathrm{gen}} = -\mathbf{G}^{\mathrm{T}}\tilde{\mathbf{P}}\mathbf{G} \tag{48}$$

where $\tilde{\mathbf{P}}$ is the solution to the Lyapunov equation

$$[\mathbf{A} + \mathbf{B}\tilde{\mathbf{K}}\mathbf{C}]^{\mathrm{T}}\tilde{\mathbf{P}} + \tilde{\mathbf{P}}[\mathbf{A} + \mathbf{B}\tilde{\mathbf{K}}\mathbf{C}] + \tilde{\mathbf{Q}}(\tilde{\mathbf{K}}) = \mathbf{0}. \tag{49}$$

To optimize $\tilde{\mathbf{K}}$, we use a gradient descent method. It should be noted that $\bar{P}_{\mathrm{gen}}$ in equation (48) is non-convex in $\tilde{\mathbf{K}}$, and in general there may be multiple local minima. One of the challenges associated with this problem is the choice of the initial condition for the algorithm. A study by Cai and Lim [28] suggest that the initial guess should be

$$\tilde{\mathbf{K}}_0 = \mathbf{K}\mathbf{C}^{\mathrm{T}} \tag{50}$$

where $\mathbf{K}$ is the solution to the full-state Riccati equation in equation (28). For the examples presented in this paper, this particular initial guess always resulted in stable closed-loop dynamics. We now present a theorem which defines the gradient of the performance with respect to the gain matrix $\tilde{\mathbf{K}}$. This is a standard result from linear-quadratic control theory and its proof can be found in [29].

Theorem 3. *The performance J in equation (46) is minimized by*

$$\frac{\partial J}{\partial \tilde{\mathbf{K}}} = 2\left(\mathbf{B}^{\mathrm{T}}\tilde{\mathbf{P}} + \frac{1}{2}\mathbf{B}^{\mathrm{T}} + R\tilde{\mathbf{K}}\mathbf{C}\right)\boldsymbol{\Sigma}\mathbf{C}^{\mathrm{T}} = \mathbf{0} \tag{51}$$

where $\tilde{\mathbf{P}}$ is the solution to the Lyapunov equation in equation (49) and where $\boldsymbol{\Sigma}$ is the solution to another Lyapunov equation; i.e.,

$$[\mathbf{A} + \mathbf{B}\tilde{\mathbf{K}}\mathbf{C}]\boldsymbol{\Sigma} + \boldsymbol{\Sigma}[\mathbf{A} + \mathbf{B}\tilde{\mathbf{K}}\mathbf{C}]^{\mathrm{T}} + \mathbf{G}\mathbf{G}^{\mathrm{T}} = \mathbf{0}. \tag{52}$$

This theorem leads to a simple first-order gradient method for optimizing $\tilde{\mathbf{K}}$, consisting of the following steps for iteration i.

(i) Start with $\tilde{\mathbf{K}}_0 = \mathbf{K}\mathbf{C}^{\mathrm{T}}$ as the initial guess.
(ii) For a matrix $\tilde{\mathbf{K}}_i$, evaluate $\partial J/\partial \tilde{\mathbf{K}}$ as in equation (51).
(iii) Compute $\tilde{\mathbf{K}}_{i+1}$ by updating $\tilde{\mathbf{K}}_i$ in the direction of the steepest descent, with a user-specified step size ϵ, as

$$\tilde{\mathbf{K}}_{i+1} = \tilde{\mathbf{K}}_i - \epsilon \left.\frac{\partial J}{\partial \tilde{\mathbf{K}}}\right|_{\tilde{\mathbf{K}}_i}. \tag{53}$$

(iv) Return to (ii) with $i \leftarrow i + 1$ until convergence is reached.

Since the focus of this study is restricted to single-transducer energy harvesting systems, the efficiency of the optimization algorithm is of little concern. The gradient descent algorithm converges to a local solution in J in 10–20 iterations for the examples discussed later in this paper. This is likely due to the fact that the initial guess $\tilde{\mathbf{K}}_0$ is close to a local minimum. A more robust method for systems with an arbitrary number of transducers is presented in [30]. The algorithm used in that study involves solving linear matrix inequalities within a scaled min/max optimization routine.

A special case of partial-state feedback arises when only the transducer voltage is used to determine the current command $i(t)$. In other words, the electronics are implementing a static admittance where $i(t) = -\tilde{K}_{\mathrm{v}}v(t)$ by convention. Because the system only has one design parameter (i.e., $\tilde{K}_{\mathrm{v}}$) in this case, the most straightforward way to optimize $\bar{P}_{\mathrm{gen}}$ is via a one-dimensional line search. One can, for example, employ the bisection algorithm instead of the gradient descent method to converge rapidly to the optimal $\tilde{K}_{\mathrm{v}}$, given $\mathbf{A}$, $\mathbf{B}$, $\mathbf{G}$, and R.

6. Simulation examples

The ratio of $\bar{P}_{\mathrm{gen}}$ for optimal static voltage feedback, over the value of $\bar{P}_{\mathrm{gen}}$ with optimal state feedback, gives us an idea of the potential for improvement in energy harvesting performance. For clarity, let $\bar{P}^{f}_{\mathrm{gen}}$, $\bar{P}^{y}_{\mathrm{gen}}$, and $\bar{P}^{v}_{\mathrm{gen}}$ be the optimal values under full-state, static partial-state, and static velocity feedback, respectively. We will refer to various ratios of these three quantities, for example, as $\rho^{vf} = \bar{P}^{v}_{\mathrm{gen}}/\bar{P}^{f}_{\mathrm{gen}}$. Analogous conventions hold for other ratios.

6.1. ρ^{vf} when the Riccati equation decouples

We first present results illustrating ρ^{vf} for the case when the Riccati equation decouples for both the electromagnetic and piezoelectric energy harvesting examples. Figure 4 shows ρ^{vf} for the electromagnetic energy harvester for various values of d and R, and for ranges of $\zeta_{\mathrm{a}} \in [0, 1]$. Similarly, figure 5 shows ρ^{vf} for the piezoelectric energy harvester for various values of d, β, and R, and for ranges of $\zeta_{\mathrm{a}} \in [0, 1]$. From these plots we see that there is a finite bandwidth for $a(t)$ at which knowledge of the derivative of the harvester states together with the disturbance acceleration is most beneficial. For the electromagnetic harvester, we see that knowledge of these states greatly improves performance over the entire range of ζ_{a} values for the asymptotic case where $R \to 0$. However, this is not true for the piezoelectric harvester as we see that ρ^{vf} appears to bend upwards after it reaches a minimal value.

For the piezoelectric example we observed that qualitatively, if only the voltage and acceleration states are measured (but not the velocity) and their respective feedback gains

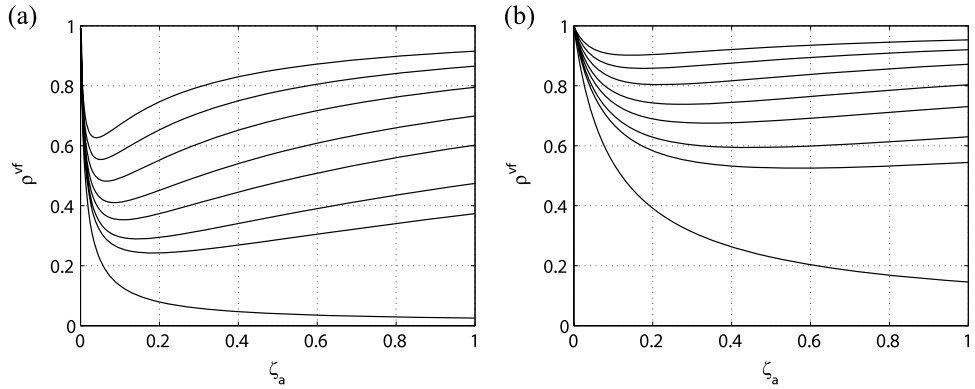

Figure 4. ρ^{vf} for the electromagnetic energy harvester, for R values of 0, 0.05, 0.08, 0.14, 0.22, 0.37, 0.61, 1 (from bottom to top): (a) $d = 0.01$; (b) $d = 0.1$.

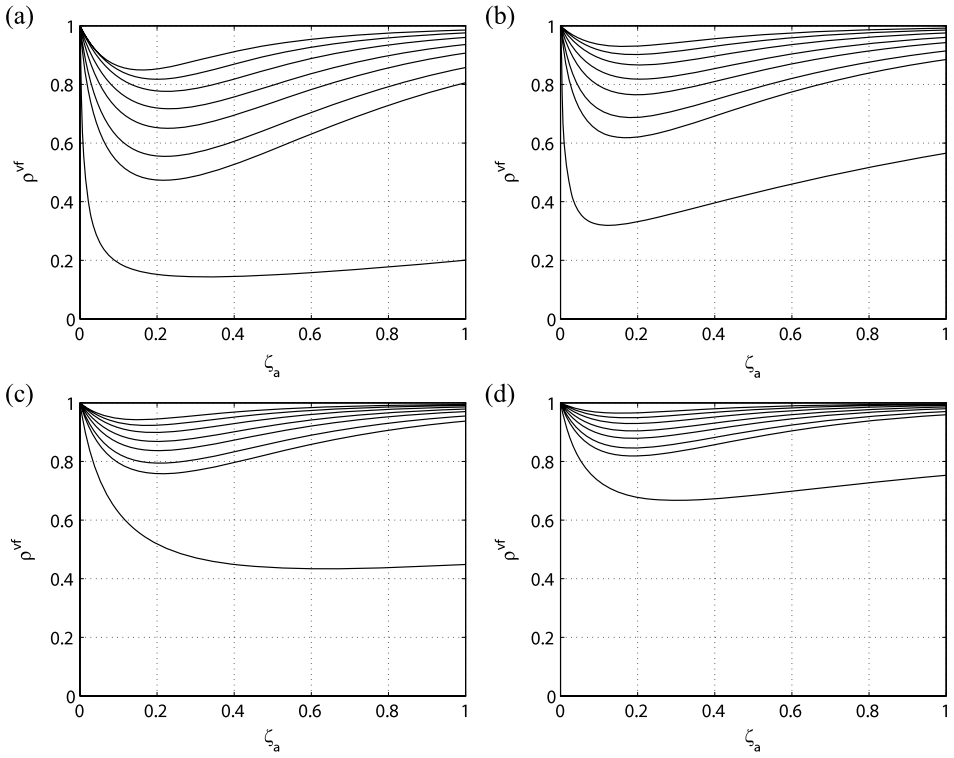

Figure 5. ρ^{vf} for the piezoelectric energy harvester, for R values of 0, 0.05, 0.08, 0.14, 0.22, 0.37, 0.61, 1 (from bottom to top): (a) $d = 0.01$ and $\beta = 0.01$; (b) $d = 0.01$ and $\beta = 0.1$; (c) $d = 0.1$ and $\beta = 0.01$; (d) $d = 0.1$ and $\beta = 0.1$.

are optimized, very little performance is sacrificed. This observation is useful because in many applications it may be advantageous to make power generation decisions without explicit knowledge of beam velocity.

6.2. Improved $\bar{P}_{\text{gen}}$ performance by tuning α

For the piezoelectric energy harvester, we have shown several benefits in terms of $\bar{P}_{\text{gen}}$ for setting α is equal to unity. However, it is possible to tune α such that the full-state feedback gains result in additional improvement in $\bar{P}_{\text{gen}}$. By tuning α to maximize $\bar{P}_{\text{gen}}$, the solution to the Riccati equation may not always decouple. The plots in figure 6 are surfaces that show the value of α that optimizes the power generation performance over the $\{\zeta_a, R\}$ domain for increasing values of mechanical damping. This plot illustrates the dependency of the optimal α surface on d. It was found that α is much more sensitive to changes in d than β.

It is interesting to note that there are three regions for values of α in these plots. The regions have distinct boundaries because, for given values of R and ζ_a, $\bar{P}_{\text{gen}}$ has two local maxima over the range of possible α values. For low levels of mechanical damping there is a region where high values α, corresponding to lower inductance values, results in the optimal performance. This region decreases in size as d increases, and eventually becomes a region where the optimal performance is obtained by setting $\alpha = 0$; i.e., the case with no inductor. In addition, for low levels of mechanical

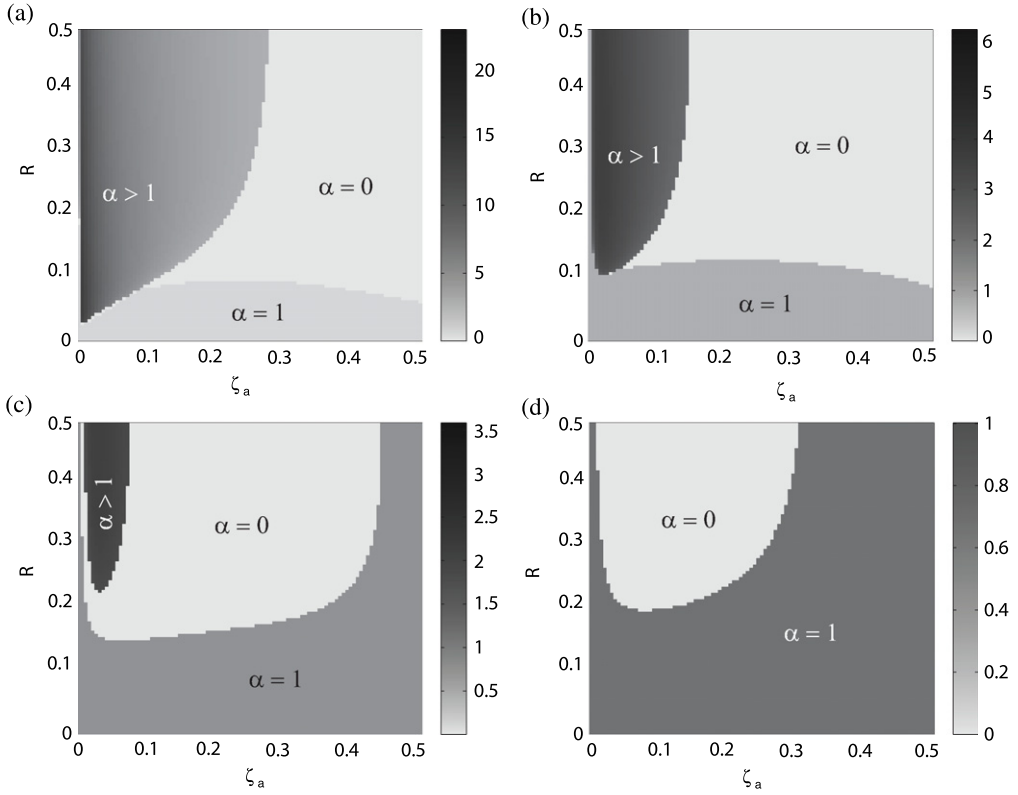

Figure 6. Optimal α values that optimize the full-state power generation performance: (a) $d = 0.01$ and $\beta = 0.01$; (b) $d = 0.04$ and $\beta = 0.01$; (c) $d = 0.07$ and $\beta = 0.01$; (d) $d = 0.1$ and $\beta = 0.01$.

damping there is a region where $\alpha = 1$ results in the optimal performance. This region occurs in an area corresponding to low levels of R, which means that the decoupling of the Riccati equation results in the optimal performance for systems with efficient electronics.

6.3. Piezoelectric energy harvester without an inductor

Finally, we consider an example where the piezoelectric energy harvester in figure 2(b) does not have an inductor connected in parallel to the terminals of its patches; i.e., $\alpha = 0$. The nondimensionalized augmented harvester and disturbance dynamics can be expressed as

$$\mathbf{A} = \begin{bmatrix} 0 & 1 & 0 & 0 & 0 \\ -1 & -d & -1 & 0 & 1 \\ 0 & 1 & -\beta & 0 & 0 \\ 0 & 0 & 0 & 0 & 1 \\ 0 & 0 & 0 & -1 & -2\zeta_a \end{bmatrix}, \quad \mathbf{B} = \begin{bmatrix} 0 \\ 0 \\ 1 \\ 0 \\ 0 \end{bmatrix}, \quad \mathbf{G} = \begin{bmatrix} 0 \\ 0 \\ 0 \\ 0 \\ 2\sqrt{\zeta_a} \end{bmatrix}. \tag{54}$$

In this case, the solution to the Riccati equation does not decouple and all of the states are required for feedback to obtain the upper bound on $\bar{P}_{\text{gen}}$. However, it is possible to improve upon the performance obtained from just feeding back voltage by feeding back voltage and disturbance acceleration. This can be accomplished by optimizing the partial-state feedback gains. For this case we define $\mathbf{C}$ as

$$\mathbf{C} = \begin{bmatrix} 0 & 0 & 1 & 0 & 0 \\ 0 & 0 & 0 & 0 & 1 \end{bmatrix} \tag{55}$$

and implement the gradient descent method to determine $\tilde{\mathbf{K}}$.

The plots in figure 7 illustrate the improvement in performance through the use of partial-state feedback gains. Figure 7(a) shows ρ^{vf}, while figure 7(b) shows ρ^{yf}. We see that including the disturbance acceleration state and optimizing the partial-state feedback gains greatly improves the power generation performance for all values of R over the range of ζ_a.

7. Conclusions

The primary purpose of this paper has been to investigate the potential for enhanced energy harvesting performance from stochastic disturbances, through the use of a partial-state feedback control law. It turns out that if the state space system describing the augmented harvester and disturbance dynamics can be expressed as being self-dual, with the harvester dynamics being WSPR, then the Riccati equation decouples. This leads to an energy harvesting current relationship that only requires half of the states for feedback. We have shown that for both electromagnetic harvesters and piezoelectric harvesters with appropriate electrical networks, the states required for feedback are the easiest to measure. The main result of this study is that more average power can be harvested with the electronics implementing the optimal

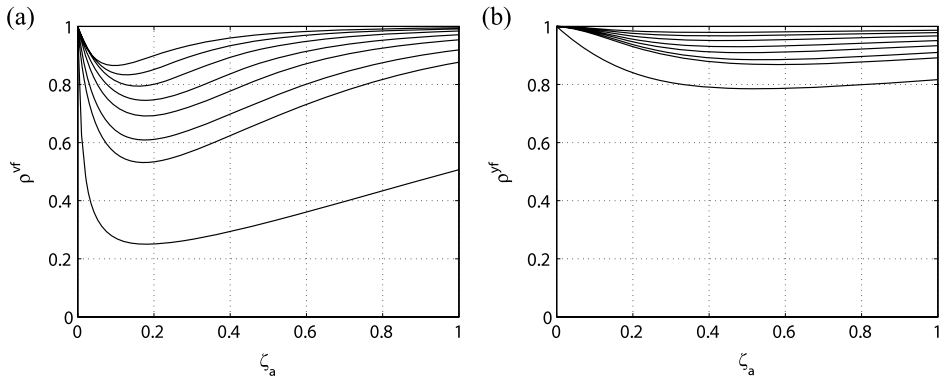

Figure 7. Comparison of the static and partial-state $\bar{P}_{\text{gen}}$ ratios, for $d = \beta = 0.01$ and for R values of 0, 0.05, 0.08, 0.14, 0.22, 0.37, 0.61, 1 (from bottom to top): (a) ρ^{vf}; (b) ρ^{yf}.

partial-state feedback control law than by implementing the optimal static admittance. This result is illustrated for both the electromagnetic and piezoelectric energy harvesters via ratios of optimal $\bar{P}_{\text{gen}}$ values obtained under different feedback assumptions.

Two additional scenarios were considered to illustrate the improvement in $\bar{P}_{\text{gen}}$ for the piezoelectric energy harvester. First, we showed that $\bar{P}_{\text{gen}}$ can be further enhanced by tuning the size of the inductor. It was found that for various levels of mechanical damping, and over the $\{\zeta_{\text{a}}, R\}$ domain, that there are three distinct regions where various inductor values optimizes $\bar{P}_{\text{gen}}$. Two of the regions correspond to cases where the Riccati does and does not decouple while the third region corresponds to the case where there is no inductor. Next, the improvement in the $\bar{P}_{\text{gen}}$ using the partial-state gradient descent routine was investigated when the piezoelectric energy harvester is not connected to an inductor. Despite the Riccati equation not decoupling, we illustrate the benefits in terms of the $\bar{P}_{\text{gen}}$ ratio for including the disturbance acceleration in addition to voltage measurements in the energy harvesting current relationship. We show for various values of R, and over the range of ζ_{a}, that the $\bar{P}_{\text{gen}}$ ratio is increased by optimizing the voltage and disturbance acceleration gains.

The analysis conducted in this paper has some limitations, which if overcome, will result in a higher degree of realism. In particular, the loss model of the power electronics was taken to consist of resistive transmission losses. This is a fairly significant simplification of the true losses incurred by an active drive, which will also include static power consumption necessary to implement the control and switch the MOSFETs, as well as significant nonlinear conductive dissipation. These dissipations will need to be addressed in order to draw clearer conclusions regarding, for example, the preferability of controlled high-frequency switched power electronics, over uncontrolled non-switching power electronics. The augmentation of the theory presented here, to include this enhanced realism, is currently underway by the authors.

Acknowledgments

Work by the first two authors was supported by NSF award CMMI-0747563. The views expressed in this article are those of the authors, and do not necessarily reflect those of the National Science Foundation.

Appendix A. Notation

$\mathbf{A}$	Augmented dynamics matrix
a	Disturbance acceleration
$\mathbf{B}$	Augmented control input matrix
b	Harvester damping
$\mathbf{C}$	Augmented output matrix
C_p	Piezoelectric equivalent capacitance
c_{e}	Electromagnetic coupling factor
$\mathbf{D}$	Damping matrix
d	Mechanical damping coefficient
$\mathbf{G}$	Augmented disturbance input matrix
i	Control current
$\mathbf{K}$	Optimal full-state gain matrix
$\tilde{\mathbf{K}}$	Optimal partial-state gain matrix
K_{a}	Optimal static acceleration gain
$K_{\dot{r}}$	Optimal static velocity gain
K_{v}	Optimal static voltage gain
$\tilde{K}_{\text{v}}$	Optimal static admittance
k	Harvester stiffness
L	Piezoelectric harvester inductance
m	Harvester mass
$\mathbf{P}$	Riccati equation solution
$\tilde{\mathbf{P}}$	Partial-state feedback Lyapunov equation solution
$\bar{P}_{\text{gen}}$	Average power generation
P_{s}	Power delivered to storage
R	Effective resistance of the electronics
R_p	Piezoelectric dielectric leakage resistance
r	Harvester relative displacement
$\mathbf{S}$	Stiffness matrix
V_{s}	Storage voltage
v	Harvester voltage
w	White noise process
$\mathbf{x}$	Augmented state vector
α	Electrical and mechanical natural frequencies squared
β	Electrical damping coefficient
Γ	Piezoelectric beam equivalent mass
ζ_{a}	Disturbance filter damping factor
θ	Piezoelectric coupling factor
λ	Piezoelectric flux linkage
Σ	Covariance matrix
σ_{a}	Disturbance standard deviation

Φ_a Disturbance power spectral density
ω_a Disturbance filter natural frequency
$\mathcal{E}$ Expectation operator

Appendix B. Proof of theorem 2

We start by defining the unique, stabilizing solution to the Riccati equation in equation (28) as

$$\mathbf{P} = \begin{bmatrix} \mathbf{P}_1 & \mathbf{P}_2 \\ \mathbf{P}_2^{\mathrm{T}} & \mathbf{P}_3 \end{bmatrix} \tag{56}$$

where

$$\mathbf{P}_1 = \begin{bmatrix} \mathbf{P}_{11} & \mathbf{P}_{12} \\ \mathbf{P}_{12}^{\mathrm{T}} & \mathbf{P}_{22} \end{bmatrix}, \tag{57}$$

$$\mathbf{P}_2 = \begin{bmatrix} \mathbf{P}_{13} & \mathbf{P}_{14} \\ \mathbf{P}_{23} & \mathbf{P}_{24} \end{bmatrix}, \tag{58}$$

$$\mathbf{P}_3 = \begin{bmatrix} \mathbf{P}_{33} & \mathbf{P}_{34} \\ \mathbf{P}_{34}^{\mathrm{T}} & \mathbf{P}_{44} \end{bmatrix}. \tag{59}$$

Thus, for the augmented state space system in equation (5), the Riccati equation can be expanded into three coupled equations in $\mathbf{P}_1$, $\mathbf{P}_2$, and $\mathbf{P}_3$; i.e.,

$$\mathbf{P}_1\mathbf{A}_h + \mathbf{A}_h^{\mathrm{T}}\mathbf{P}_1 - \frac{1}{R}\left(\mathbf{P}_1 + \frac{1}{2}\mathbf{I}\right)\mathbf{B}_h\mathbf{B}_h^{\mathrm{T}}\left(\mathbf{P}_1 + \frac{1}{2}\mathbf{I}\right) = \mathbf{0}, \tag{60}$$

$$\mathbf{P}_1\mathbf{G}_h\mathbf{C}_a + \mathbf{P}_2\mathbf{A}_a + \mathbf{A}_h^{\mathrm{T}}\mathbf{P}_2 - \frac{1}{R}\left(\mathbf{P}_1 + \frac{1}{2}\mathbf{I}\right)\mathbf{B}_h\mathbf{B}_h^{\mathrm{T}}\mathbf{P}_2 = \mathbf{0}, \tag{61}$$

$$\mathbf{P}_2^{\mathrm{T}}\mathbf{G}_h\mathbf{C}_a + \mathbf{C}_a^{\mathrm{T}}\mathbf{G}_h^{\mathrm{T}}\mathbf{P}_2 + \mathbf{P}_3\mathbf{A}_a + \mathbf{A}_a^{\mathrm{T}}\mathbf{P}_3 - \frac{1}{R}\mathbf{P}_2^{\mathrm{T}}\mathbf{B}_h\mathbf{B}_h^{\mathrm{T}}\mathbf{P}_2 = \mathbf{0}. \tag{62}$$

As discussed in [8], if the harvester is WSPR, then equation (60) has a unique solution $\mathbf{P}_1$ which is stabilizing (i.e., for which $\mathbf{A}_h - \frac{1}{R}\mathbf{B}_h^{\mathrm{T}}(\mathbf{P}_1 + \frac{1}{2}\mathbf{I})$ is asymptotically stable), and for which $\mathbf{P}_1 + \frac{1}{2}\mathbf{I} > 0$ is a closed-loop Lyapunov matrix for the free response of the controlled harvester (i.e., with $a(t) = 0$). It only remains to show that the decoupled solution above is in fact the stabilizing one. Defining $\bar{\mathbf{P}}_1 = \mathbf{P}_1 + \frac{1}{2}\mathbf{I}$, equation (60) becomes

$$-\frac{1}{2}(\mathbf{A}_h + \mathbf{A}_h^{\mathrm{T}}) + \bar{\mathbf{P}}_1\mathbf{A}_h + \mathbf{A}_h^{\mathrm{T}}\bar{\mathbf{P}}_1 - \frac{1}{R}\bar{\mathbf{P}}_1\mathbf{B}_h\mathbf{B}_h^{\mathrm{T}}\bar{\mathbf{P}}_1 = \mathbf{0}. \tag{63}$$

For the case where $\mathbf{A}_h$ and $\mathbf{B}_h$ satisfy equation (30), then it is straightforward to verify that a solution to equation (63) is $\bar{\mathbf{P}}_{11} = \bar{\mathbf{P}}_{22} = \bar{\mathbf{P}}_{22}^{\mathrm{T}}$ and $\bar{\mathbf{P}}_{12} = \mathbf{0}$ where $\bar{\mathbf{P}}_{22}$ can be found by solving the Riccati equation

$$\frac{1}{2}(\mathbf{D}+\mathbf{D}^{\mathrm{T}}) + \bar{\mathbf{P}}_{22}(-\mathbf{D}) + (-\mathbf{D})^{\mathrm{T}}\bar{\mathbf{P}}_{22} - \frac{1}{R}\bar{\mathbf{P}}_{22}\mathbf{B}_1\mathbf{B}_1^{\mathrm{T}}\bar{\mathbf{P}}_{22} = \mathbf{0} \tag{64}$$

which is equivalent to equation (33) for $\mathbf{P}_1$. Now, it is a fact that $(-\mathbf{D}, \mathbf{D} + \mathbf{D}^{\mathrm{T}})$ is observable if $(\mathbf{A}_h, \mathbf{A}_h + \mathbf{A}_h^{\mathrm{T}})$ is. This follows from the fact that if $\mathbf{v}$ is an eigenvector of $\mathbf{A}_h$ with eigenvalue η with $\Re\{\eta\} < 0$, then it must have the structure $\mathbf{v} = [\mathbf{v}_1^{\mathrm{T}}\ \eta\mathbf{v}_1^{\mathrm{T}}]^{\mathrm{T}}$, which, in turn, implies that $\mathbf{v}_1$ is an eigenvector of $-\mathbf{D}$, with associated eigenvalue $\eta_1 = \eta + 1/\eta$. If $(-\mathbf{D}, \mathbf{D} + \mathbf{D}^{\mathrm{T}})$ were unobservable, that would require that at least one such $\mathbf{v}_1$ satisfy $(\mathbf{D} + \mathbf{D}^{\mathrm{T}})\mathbf{v}_1 = \mathbf{0}$, but this would also require that the corresponding $\mathbf{v}$ satisfy $(\mathbf{A}_h + \mathbf{A}_h^{\mathrm{T}})\mathbf{v} = \mathbf{0}$, which violates the WSPR assumption. By contradiction, we conclude that $(-\mathbf{D}, \mathbf{D} + \mathbf{D}^{\mathrm{T}})$ is observable. Furthermore, in the process we have shown that $-\mathbf{D}$ is asymptotically stable, because if $\Re\{\eta\} < 0$ then $\Re\{\eta_1\} = \Re\{\eta\} + \Re\{1/\eta\} < 0$. But if $-\mathbf{D}$ is asymptotically stable, $(-\mathbf{D}, \mathbf{D} + \mathbf{D}^{\mathrm{T}})$ is observable, and $R > 0$, then equation (64) is a standard Riccati equation with a unique stabilizing solution $\bar{\mathbf{P}}_{22} = \bar{\mathbf{P}}_{22}^{\mathrm{T}} > 0$ [31]. Consequently, we have that there is a corresponding unique stabilizing solution $\mathbf{P}_{22} = \mathbf{P}_{22}^{\mathrm{T}}$ to equation (33), and that the corresponding decoupled solution for $\mathbf{P}_1 = \mathbf{P}_1^{\mathrm{T}}$ in equation (60) is the stabilizing solution.

Now, as shown in [8], the other components of $\mathbf{P}$ are found uniquely, once $\mathbf{P}_1$ is found. Using the decoupled result obtained for $\mathbf{P}_1$ and substituting $\mathbf{A}_a$ and $\mathbf{C}_a$ as defined in equation (31) into equation (61) results in $\mathbf{P}_{14} = \mathbf{P}_{23} = \mathbf{0}$. In addition, we have that $\mathbf{P}_{13} = \mathbf{P}_{24}$ where $\mathbf{P}_{24}$ can be found by solving equation (34). With $\mathbf{P}_1$ and $\mathbf{P}_2$ solved and the decoupled expression for $\mathbf{P}_2$ substituted into equation (62), we have that $\mathbf{P}_{34} = \mathbf{0}$ and $\mathbf{P}_{33} = \mathbf{P}_{44}$ where $\mathbf{P}_{44}$ is the solution to equation (35). See [8] for the proof that $\mathbf{P}_3 < 0$. Substituting the decoupled solution for $\mathbf{P}$ into equation (27) gives equation (36) immediately. Finally, substituting the decoupled form for $\mathbf{P}$ into the expression for the upper bound on the average power generated results in equation (37).

References

[1] Roundy S, Wright P K and Rabaey J 2002 A study of low level vibrations as a power source for wireless sensor nodes *J. Comput. Commun.* **26** 1131–44

[2] Beeby S P, Tudor M J and White N M 2006 Energy harvesting vibration sources for microsystems applications *Meas. Sci. Technol.* **17** R175–95

[3] Anton S R and Sodano H A 2007 A review of power harvesting using piezoelectric materials (2003–2006) *Smart Mater. Struct.* **16** R1–21

[4] Knight C, Davidson J and Behrens S 2008 Energy options for wireless sensor nodes *Sensors* **8** 8037–66

[5] Kasyap A, Lim J, Johnson D, Horowitz S, Nishida T, Ngo K, Sheplak M and Cattafesta L 2002 Energy reclamation from a vibrating piezoceramic composite beam *9th Int. Congr. on Sound and Vibration (Orlando, FL, July 2002)*

[6] Lefeuvre E, Audigier D, Richard C and Guyomar D 2007 Buck-boost converter for sensorless power optimization of piezoelectric energy harvester *IEEE Trans. Power Electron.* **22** 2018–25

[7] Kong N, Ha D S, Erturk A and Inman D J 2010 Resistive impedance matching circuit for piezoelectric energy harvesting *J. Intell. Mater. Syst. Struct.* **21** 1293–302

[8] Scruggs J T 2010 On the causal power generation limit for a vibratory energy harvester in broadband stochastic response *J. Intell. Mater. Syst. Struct.* **21** 1249–62

[9] Ottman G K, Hofmann H F and Lesieutre G A 2003 Optimized piezoelectric energy harvesting circuit using step-down converter in discontinuous conduction mode *IEEE Trans. Power Electron.* **18** 696–703

[10] Stephen N G 2006 On energy harvesting from ambient vibration *J. Sound Vib.* **293** 409–25

[11] Lefeuvre E, Badel A, Richard D and Guyomar D 2005 Piezoelectric energy harvesting device optimization by synchronous electric charge extraction *J. Intell. Mater. Syst. Struct.* **16** 865–7

[12] Badel A, Guyomar D, Lefeuvre E and Richard D 2005 Efficiency enhancement of a piezoelectric energy harvesting device in pulsed operation by synchronous charge inversion *J. Intell. Mater. Syst. Struct.* **16** 889–901

[13] Guyomar D, Badel A, Lefeuvre E and Richard D 2005 Toward energy harvesting using active materials and conversion improvement by nonlinear processing *IEEE Trans. Ultrason., Ferroelectr., Freq. Control* **52** 584–95

[14] Burrow S G and Clare L R 2009 Open-loop power conditioning for vibration energy harvesters *Electron. Lett.* **45** 999–1000

[15] Adhikari S, Friswell M and Inman D J 2009 Piezoelectric energy harvesting from broadband random vibrations *Smart Mater. Struct.* **18** 115005

[16] Main J A, Newton D V, Massengill L and Garcia E 1996 Efficient power amplifiers for piezoelectric applications *Smart Mater. Struct.* **5** 766–75

[17] Chandrasekaran S, Lindner D K and Smith R C 2000 Optimized design of switching amplifiers for piezoelectric actuators *J. Intell. Mater. Syst. Struct.* **11** 887–901

[18] Liu Y, Tian G, Wang Y, Lin J, Zhang Q and Hofmann H F 2009 Active piezoelectric energy harvesting: general principle and experimental demonstration *J. Intell. Mater. Syst. Struct.* **20** 575–85

[19] Scruggs J T 2009 An optimal stochastic control theory for distributed energy harvesting networks *J. Sound Vib.* **320** 707–25

[20] Ward J K and Behrens S 2008 Adaptive learning algorithms for vibration energy harvesting *Smart Mater. Struct.* **17** 035025

[21] Kassakian J, Schlecht M and Verghese G 1991 *Principles of Power Electronics* (Reading, MA: Addison-Wesley)

[22] Scruggs J T and Cassidy I L 2010 Optimal and sub-optimal power management in broadband vibratory energy harvesters with one-directional power flow constraints *SPIE Int. Symp. on Smart Materials and Structures/NDE (San Diego, CA, March 2010)*

[23] Brogliato B, Lozano R, Maschke B and Egeland O 2007 *Dissipative Systems Analysis and Control* (London: Springer)

[24] Lozano-Leal R and Joshi S M 1988 On the design of dissipative lqg type controller *IEEE Conf. on Decision and Control (Austin, TX, Dec. 1988)*

[25] Glynne-Jones P, Tudor M J, Beeby S P and White N M 2004 An electromagnetic, vibration-powered generator for intelligent sensor systems *Sensors Actuators* A **110** 344–9

[26] Scruggs J T and Behrens S 2011 Optimal energy harvesting from low-frequency bistate force loadings *J. Vib. Acoust.* **133** 011008

[27] Luenberger D G 1971 An introduction to observers *IEEE Trans. Autom. Control* **16** 596–602

[28] Cai G P and Lim C W 2005 Continuous suboptimal control with partial state feedback *J. Vib. Control* **11** 561–78

[29] Dorato P, Abdallah C T and Cerone V 1995 *Linear-Quadratic Control* (Englewood Cliffs, NJ: Prentice Hall)

[30] Iwasaki T, Skelton R E and Geromel J C 1994 Linear quadratic suboptimal control with static output feedback *Syst. Control Lett.* **23** 421–30

[31] Bernstein D S 2009 *Matrix Mathematics* (Princeton, NJ: Princeton University Press)